THE ASTROPHYSICAL JOURNAL, 427:174–183, 1994 May 20

GALAXIES WITH EXTREME INFRARED AND Fe II EMISSION. I. MARKARIAN 231: THE SIGNATURE OF A YOUNG INFRARED QSO

SEBASTIAN LÍPARI[1,2]
Space Telescope Science Institute, 3700 San Martin Drive, Baltimore, MD 21218; lipari@stsci.edu
LUIS COLINA[2]
Departamento de Fisica Teorica, Universidad Autonoma, Madrid, Spain; colina@stsci.edu
AND
F. MACCHETTO[3]
Space Telescope Science Institute, 3700 San Martin Drive, Baltimore, MD 21218; macchetto@stsci.edu
Received 1992 December 2; accepted 1993 November 17

ABSTRACT

We investigate the ultraluminous IR Galaxy/QSO Mrk 231 by means of long-slit optical spectroscopy, high spatial resolution broad-band optical imaging and UV *IUE* spectra. The spectrum shows an extreme Fe II optical emission ($Fe\ II_{OPT}/H\beta \approx 8$), broad Balmer and Na ID lines, weak high-excitation lines, double-peaked optical narrow emission lines with velocity differences of about 1000 km s^{-1}, a steep UV spectrum, and a weak Lyα line. These spectral features are explained "mainly" by the presence of nuclear and circumnuclear starbursts. The high spatial resolution broad-band images show details of two interesting blue circumnuclear subregions, in particular: (1) a blue region 2″–5″ west of the nucleus; and (2) a blue arc ("horseshoe") at ~3″.5 S.

In "region I" (circumnuclear star-forming region located at ~2″–5″ to the west from the nucleus) we detect an emission-line system (E0) with a velocity ($V_{E0} = 7941 \pm 80$ km s^{-1}) similar to that of the nuclear system BAL1 ($V_{BAL1} \sim 7800$ km s^{-1}), the strongest of the three broad absorption-line systems. Moreover, in this region we also detect the probable presence of this BAL1 system ($V_{NaID} = 7840 \pm 120$ km s^{-1}). Consequently, Mrk 231 is the first candidate where a direct link, at least kinematical, between a star-formation process and the BAL phenomenon is observed.

We discuss *physical, kinematic and morphological* evidence of a strong nuclear and circumnuclear starburst (with superwind/superbubble and supernova of Type II), in Mrk 231. These results and studies are consistent with a scenario where this ultraluminous IR galaxy has a composite nature in the nuclear region, which is the consequence of the final phases of an ongoing merger process. The starburst is the *dominant* source of nuclear energy and the nonthermal active galactic nuclei remains strongly obscured. We also discuss the extreme properties of Mrk 231 as the probable characteristics/signature typical of a young IR QSO.

Subject headings: galaxies: individual (Markarian 231) — galaxies: kinematics and dynamics — galaxies: nuclei — galaxies: stellar content — infrared: galaxies — quasars: general

1. INTRODUCTION

Observational and theoretical investigations of ultraluminous infrared (IR) galaxies ($L_{IR} \geq 10^{12}\ L_\odot$) in the last several years have provided increasing evidence that these objects represent an important phase in the *early evolution* of the activity of galaxies (Rowan-Robinson et al. 1991; Sanders et al. 1988a, b; Heckman, Armus, & Miley 1987, 1990; Hutching & Neff 1988, 1991). Moreover, different studies suggest that the physical conditions in ultraluminous IR galaxies could be very similar to those expected in protogalaxies (Heckman et al. 1990; Sanders et al. 1988a; Rowan-Robinson et al. 1991; Djorgovski & Weir 1990) and that a starburst/explosive scenario fits well with theoretical and/or observational studies of these two types of objects. Consequently, these may be excellent low-redshift analogs of galaxy-formation processes occurring at earlier epochs.

In particular, different scenarios for the formation of galaxies suggest that when a galaxy is being formed, the rate of star formation should be considerably higher than at present, and in this vigorous process some of the ionized gas may be ejected from the galactic disk by supernova explosions and stellar winds (see Heckman et al. 1990 for references). In high-luminosity IR galaxies ($L_{IR} \geq 10^{11}\ L_\odot$), studies based on the emission-line ratios, Hα radio, and IR luminosities show that these objects are places where active star formation with strong "superwinds" is taking place (see Rieke et al. 1980, 1985; Heckman et al. 1987, 1990; Armus, Heckman, & Miley 1989, 1990; Leech et al. 1989; Lípari, Bonatto, & Pastoriza 1991a; Colina & Perez-Olea 1992; Rieke 1992). Also, for IR luminosities in excess of $10^{11} L_\odot$ there is a clear increase in the nonthermal nuclear activity (Sanders et al. 1988a).

Furthermore, different surveys of ultraluminous IR galaxies show that almost 100% are interacting and active systems (Sanders et al. 1988a; Melnick & Mirabel 1990; Heckman et al. 1987). And in recent years there has been increasing evidence showing that galaxy collisions can lead to the enhancement/fueling of various kinds of nuclear activity, especially the star-

[1] Córdoba Observatory, and Conicet, Argentina.
[2] Visiting Astronomer at La Palma Observatory.
[3] Affilliated with the Astrophysics Department, Space Science Division, European Space Agency (ESA).

burst and Seyfert phenomenon (see, for reviews, Heckman 1990, 1991; Sanders 1992).

On the other hand, during the last two decades, considerable theoretical and observational effort has been devoted to understanding the Fe II emission in active galactic nuclei (AGNs) (see Joly 1991 for references); however, the nature of this emission is not yet well understood. AGNs with strong and, in particular, extremely strong Fe II emission (Fe II [37, 38] $\lambda 4570/\mathrm{H}\beta > 2$) are especially important, because the Fe II emission is one of the important parameters to test different models of AGNs. Recently, Lípari, Terlevich, & Macchetto (1993a) found that almost 100% of extremely strong Fe II emitters are ultraluminous IR AGNs and radio-quiet objects. We suggested that these objects comprise an important group of AGNs, possibly young IR QSOs[4] at the end phase of a strong starburst.

We are conducting studies of selected luminous and ultraluminous IR galaxies, especially extreme IR and Fe II emitters. The first objects studied already reveal a wealth of interesting results. For example, in IRAS 18508 − 7815 we found the first southern IR QSO with extreme Fe II emission, and we discussed the interesting properties of this small group of AGNs (Lípari, Macchetto, & Golombek 1991b). In IRAS 19254 − 7245 ("The Superantennae"), we detected and studied one of the most remarkable instances of galaxy-galaxy collision, exhibiting gigantic tails (~350 kpc!). We found an intense ongoing star-formation process with large-scale mass outflows ("superwinds") together with a hidden quasar-like nuclear source (Colina, Lípari, & Macchetto 1991). In IRAS 20044 − 6114 we detected a variable Seyfert nucleus embedded in a dusty starburst environment (Lípari, Tsvetanov, & Macchetto 1993b).

This paper reports results of our studies of individual galaxies showing extreme IR and Fe II emission, for the nearest object of this group: Mrk 231. This galaxy is an *extremely* luminous object with $M_V = -22.5$ and $M_K = -24.7$ (Rieke & Low 1972, 1975; Cutri, Rieke, & Lebofsky 1984). Moreover, in the IR, Mrk 231 is the brightest active galaxy in the local universe ($L_{\mathrm{IR}[8-1000\,\mu\mathrm{m}]} = 3.5 \times 10^{12}\ L_\odot$; see Soifer et al. 1986, 1987), with a ratio $L_{\mathrm{IR}}/L_B \sim 200$! Consequently, the bolometric luminosity–dominated by the IR continuum emission—places this galaxy among the QSOs.

Mrk 231 also shows very unusual spectral characteristics, dominated in the optical by *extremely* strong Fe II and broad Balmer emission lines (at $z_{\mathrm{em}} = 0.042$; see Arakelian et al. 1971; Adams & Weedman 1972). In addition, it shows *remarkable* absorption line systems: one clear stellar absorption (at $z_{\mathrm{abs}} \sim 0.042$) and three broad absorption line (BAL) systems (at $z_{\mathrm{BAL1}} \sim 0.026$, $z_{\mathrm{BAL2}} \sim 0.020$, and $z_{\mathrm{BAL3}} \sim 0.016$; see Arakelian et al. 1971; Adams & Weedman 1972; Adams 1972; Boksenberg et al. 1977, hereafter BEA77; Boroson et al. 1991). The optical morphology of Mrk 231 indicates a system with an irregular structure, and with the gas highly concentrated in the nuclear/circumnuclear regions (Hamilton & Keel 1987, hereafter HK87; Sanders et al. 1987, hereafter SEA87; Hutchings & Neff 1987, hereafter HN87). Furthermore, the existence of a strong OH maser source in this galaxy (Baan 1985) gives support to the idea of an *extreme starburst* in the nuclear/circumnuclear region of this system.

In the following sections (§§ 2 and 3) we present the observations and results, respectively. The interpretation of these results is discussed in § 4. Throughout the paper a Hubble constant of $H_0 = 75$ km s^{-1} Mpc^{-1} will be assumed. The distance to the galaxy is then ~168 Mpc, and the angular scale $1'' \sim 814$ pc.

2. OBSERVATIONS AND REDUCTIONS

High-resolution V broad-band CCD images were obtained in 1991 May, with the 2.5 m NOT[5] telescope at La Palma Observatory, Spain. A TEX CCD chip with a scale of 0.″197 per pixel was used. The observations were carried out in excellent seeing conditions, with a value of 0.″7 (FWHM).

Optical spectroscopic observations of Mrk 231 were obtained in 1991 February, at the 2.1 m KPNO telescope, Arizona, USA. Long-slit spectra were taken using the Gold Spectrograph with the TI 800 × 800 pixels CCD. The observations were made using a 300 lines mm^{-1} grating, with a 1.″5 slit which gives a resolution of 6.5 to 7 Å. The observations were carried out in photometric conditions, the seeing was ~1″ (FWHM).

The IRAF[6] software package was used to reduce the optical data in the standard way. Wavelength calibration of the spectra was done by fitting a two-dimensional polynomial to the position of lines in the arc frame. The spectra were flux calibrated with standard stars. The emission and absorption lines were decomposed using Gaussian profiles by means of a nonlinear least-squares algorithm described in Bevington (1969).

The UV *IUE*[7] low-resolution (~8 Å) archival data consist of two spectra (SWP 9602 and LWR 4053) obtained, respectively, on 1980 July and 1979 March with integration times of 888 and 412 minutes.

3. RESULTS

3.1. *Optical Broad-Band Morphology*

Previous studies show a classical merger morphology for this object: a distorted main body with a diameter of ~35 kpc, from which two curved tails emerge, with a total extension of ~75 kpc (see SEA87; HK87; HN87).

The high spatial resolution broad-band V images of Mrk 231 are shown in Figures 1*a*, 1*b*, and 2 (Plate 7). These images show details of two interesting blue circumnuclear regions/structures.

1. *Region I.*—Area located at ~2″–5″ to the west, from the nucleus (see Figs. 1*a* and HK87). In part of this region, we detect blue continuum and double-peaked narrow emission lines (see § 3.2.3). Ulvestad, Wilson, & Sramek (1981) present a map at 4.885 GHz showing a peak plus an extended radio emission associated with this area. Moreover, we found that the emission-line ratios for this region also show the typical characteristics of a powerful starburst/superwind. This point will be discussed in detail in §§ 3.2.3 and 4.3.

2. *Region or Structure II.*—Symmetric and extended blue arc (or "horseshoe;" see HK87) located at 3.″5 (2.9 kpc) to the south of the nucleus (Figs. 1*a* and 2). The morphology of this structure shows that this feature is possibly symmetric, with its center approximately centered on the nucleus. The internal part of this structure shows the presence of several extended

[4] Here we refer to luminous AGNs as "QSOs," to luminous radio-loud AGNs as "quasar," and to active galactic nuclei (i.e., supermassive BH and/or starburst) as "AGNs."

[5] Nordic Optical Telescope.

[6] IRAF is the imaging analysis software developed by NOAO.

[7] *International Ultraviolet Explorer* satellite.

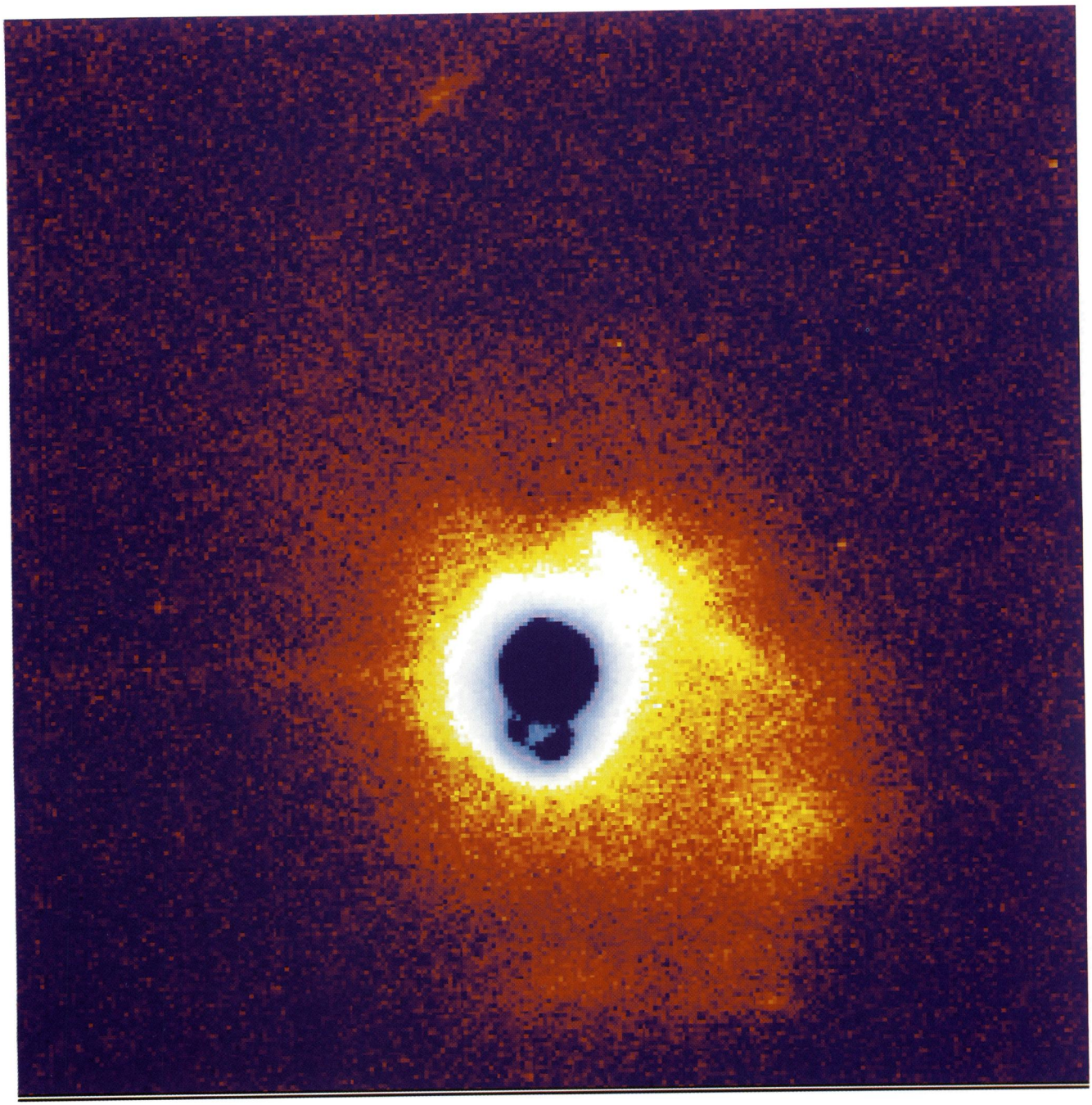

FIG. 2.—CCD V broad-band color images of Mrk 231 (52″ × 52″). North is up and east is to the left.

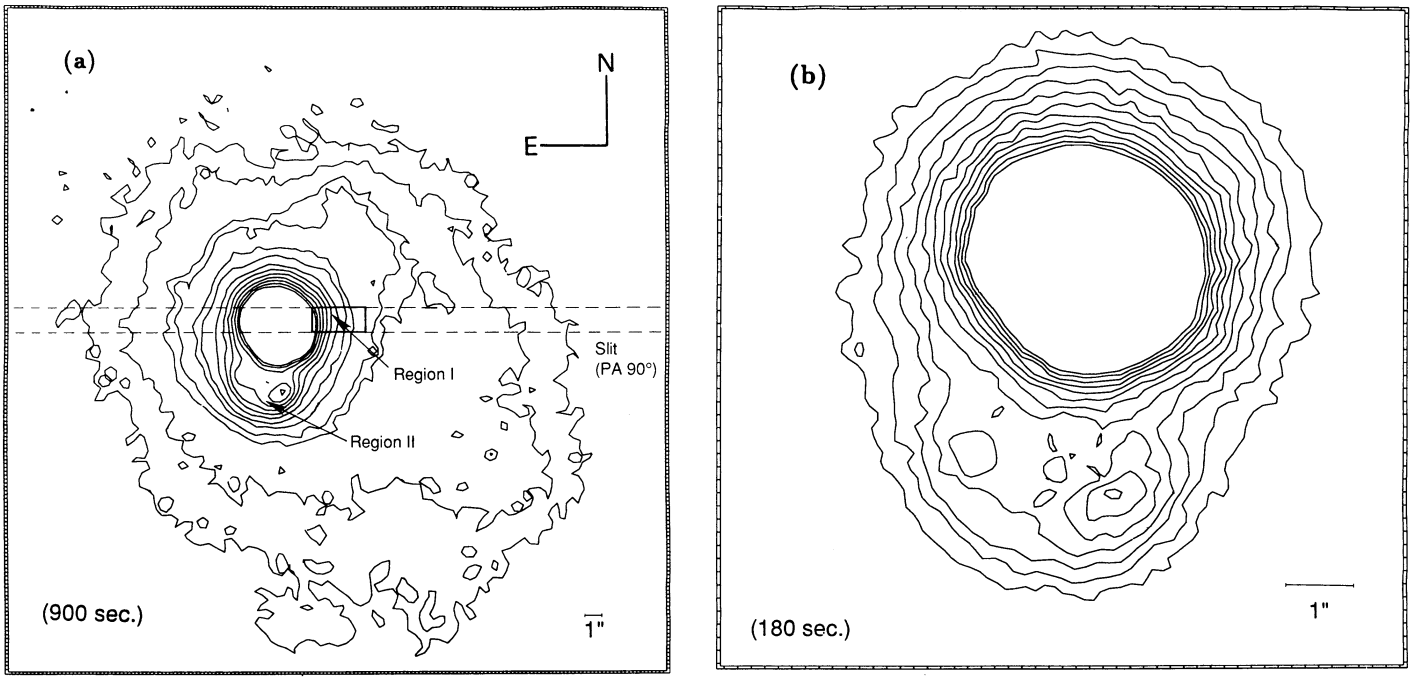

FIG. 1.—CCD V broad-band contour plots of Mrk 231 (first contours are 2 σ from the background). (*a*) Contour plot showing the general distorted morphology and the blue "regions I and II" (see the text). (*b*) Contour plot, from a short exposure image, showing in detail the "region/structure II" and the nucleus.

knots. In this region, HK87 detected blue continuum and a double-peaked [O III] λ5007 emission line (with $\Delta V_{[\mathrm{O\ III}]\lambda 5007} \sim -500$ km s^{-1}).

Furthermore, it is interesting to note that our observations with very short exposures (180 s) and better resolution (0".6 FWHM; see Fig. 1*b*) show mainly the compact nucleus and better morphological detail of structure II.

The main body of the distorted disk of Mrk 231 shows details of several extended knots associated with star-formation regions (see Figs. 1*a* and 2; HK87; HN87). In Figure 2—and even more clearly in the images of HN87, SEA87, HK87—we also show the north external tail, with details of an extended condensation (located at 23 kpc in the N direction, from the nucleus); similar to those that we found in the interacting ultraluminous IR galaxy "The Superantennae" (Colina et al. 1991). The nature of this type of condensation is likely to be related to a star-formation process (Mirabel, Dottori, & Lutz 1992; Barnes & Hernquist 1992).

3.2. *Optical Spectroscopy*

3.2.1. *The Nuclear Emission-Line Spectrum*

The "nuclear" optical spectrum of Mrk 231 (extraction of 2" centered in the nucleus and at P.A. 90°) is shown in Figure 3*a*, while the corresponding line fluxes are shown in Table 1. Also, in this table and in Figure 3*b*, we show the flux values and the nuclear spectrum corrected for internal extinction with a reddening $E(B-V) = 0.63$ (BEA77) and a LMC extinction law (Nandy et al. 1981). In addition, we fitted the continuum with a power law ($F_\nu = \nu^{-\alpha}$), and we obtain a spectral index $\alpha = 0.60 \pm 0.15$.

At optical wavelengths Mrk 231 has the spectral characteristics typical of strong Fe II emitters (Boroson & Meyers 1992; Lípari et al. 1993a). It shows strong optical Fe II multiplets with very weak high-excitation forbidden emission lines, as well as a blue asymmetry on the Hα emission line profile. However, the UV spectrum (see § 4.1 and HN87) does not show any evidence of typical QSO/Seyfert 1 UV emission lines; it mainly shows a narrow Lyα in emission and a flat continuum similar to those detected in starbursts (see § 4.1).

On the other hand, the nuclear optical spectrum of Mrk 231 shows properties which could be separated into three different systems of emission lines.

1. *System E1.*—The first—and clearest—system is dominated by Balmer (Hα, Hβ) emission lines with broad components (FWHM$_{\mathrm{H}\alpha} \sim 6000$ km s^{-1}, and FWHM$_{\mathrm{H}\beta} \sim 3000$ km s^{-1}), extremely strong optical Fe II emission (especially at λ4570 [multiplets 37, 38] and $\lambda\lambda$5100–5400 [multiplets 42, 48, 49]), and broad He I 5876 and Na I D λ5889–5895.

2. *System E2.*—The narrow [O II] λ3727 emission line shows a double-peaked profile with two components separated by about 1000 km s^{-1} (see Table 1). It is important to note that in the circumnuclear "regions I and II," the emission lines also show a double-peak "narrow" profile (see §§ 3.2.3 and 4.3 and HK87).

3. *System E3.*—We detect very narrow forbidden emission lines of [O III] λ5007, [O I] λ6300 and [S II] $\lambda\lambda$6717–6731 (see Table 1). We had observed similar very weak forbidden emission lines in the extreme Fe II emitter IRAS 18508 – 7815 (Lípari et al. 1991b, Fig. 2).

3.2.2. *The Nuclear Absorption-Line Systems*

The stellar population in the nucleus was studied in detail by BEA77. They found that hot young stars, B–A, are a good explanation for the observed Balmer absorption lines and for the optical continuum. Consequently, we fit the optical continuum of Mrk 231 using a blackbody function. We obtain a very good fit (even better that those obtained with power-law functions) for a temperature of $T_{\mathrm{eff}} \sim 10800 \pm 100$ K, corresponding to the typical value of B8–9(I-III-V) stars. This result

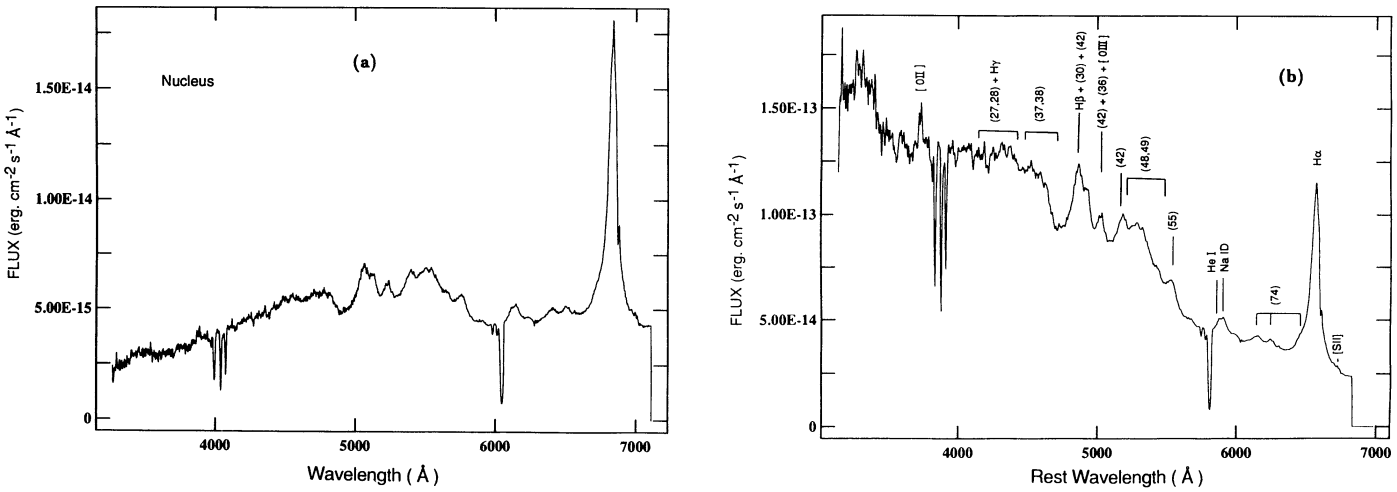

FIG. 3.—Optical nuclear spectrum of Mrk 231. (*a*) Calibrated observed spectrum. (*b*) Spectrum corrected for internal reddening and redshift. The emission line identifications are shown (numbers in brackets are multiplet numbers for Fe II emission).

is in close agreement with the conclusion of BEA77 (see also § 4.1).

The complex nature of the optical BAL systems in Mrk 231 has been discussed by various authors (BEA77; Boroson et al. 1991; Boroson & Meyers 1992), though the nature of these strong absorption lines is still not completely understood. Recently, Boroson et al. (1991) have reported significant changes in the BAL systems of this object. Our measurements, summarized in Table 2, are consistent with previous results from the above mentioned authors.

For the nuclear stellar population (see Table 2), we obtain a mean velocity of $V_{System} = 12400 \pm 150$ km s^{-1} ($cz = 12{,}670$ km s^{-1}). The presence of the new absorption system (BAL3, reported by Boroson et al. 1991) is also clear in our data.

3.2.3. *The Circumnuclear Spectra*

Adams (1972) already reported the extended nature of the [O II] λ3727 emission, for Mrk 231. In addition, BEA77 reported a double-peaked [O II] λ3727 emission feature, for the nuclear region. Inside the area called "region I" above (see

TABLE 1

NUCLEAR EMISSION LINES FLUXES

Lines	F_{obs}[a]	EW_{obs} (Å)	$FWHM_{obs}$ (Å)	F_{cor}[b]	λ_{obs} (Å)	V[c] (km s^{-1})
E1:						
Fe II (multiplet 27, 28)	50.0	121.0	310.0	480	4537.0	...
Fe II (multiplet 37, 38)	63.0	145.0	305.0	490	4735.0	...
$H\beta_B$	31.0	75.0	80.0	210	5067.0	12413
Fe II (42) λ4924	2.4	4.1	40.0	19	5131.0	12327
Fe II (42) λ5018	9.0	12.0	73.0	65	5229.0	12325
Fe II (42) λ5169	8.5	17.0	92.0	48	5400.0	...
Fe II (multiplet 48, 49)	89.0	200.0	340.0	460	5504.0	...
Fe II (55) λ5535	7.7	16.0	88.0	44	5758.0	...
He I λ5876	5.2	10.0	68.0	36	6120.0	12240
Na I D λλ5889–5895	3.5	6.5	47.0	19	6143.0	12470
Fe II (74) λ6148	7.0	15.0	90.0	26	6406.0	12327
Fe II (74) λ6248	5.5	12.3	74.0	21	6514.0	...
Fe II (74) λ6456	6.0	14.0	77.0	22	...	...
Hα	~160.0	(240.0)	(95.0)	~640	6839.0	12356
$Fe\ II_{OPT}$	248.0	...	...	1675.0	...	...
E2:						
[O II] λ3727 [blue–1]	0.5	1.7	9.8	8	3870.0	11262
[O II] λ3727 [red–2]	1.1	3.2	13.1	15	3883.5	12298
E3:						
[O III] λ5007	0.30	0.5	12.3	2	5218.7	12413
[O I] λ6300	0.10	0.2	12.1	1	6565.3	12355
[S II] λ6717	0.13	0.2	9.5	...	6998.0	12328
[S II] λ6731	0.10	0.2	9.0	...	7013.1	12327

[a] The fluxes are given in units of 10^{-14} ergs cm^{-2} s^{-1} Å^{-1}.
[b] Corrected for internal extinction (see the text) and redshift.
[c] Velocities have been obtained using the expression $1 + z = ([c + V]/[c - V])^{0.5}$.

TABLE 2

PARAMETER CHARACTERISTICS OF THE ABSORPTION LINE

Line	EW_{obs}	$FWHM_{obs}$ (Å)	λ_{obs} (Å)	V[a] (km s^{-1})	$V - V_{System}$[b] (km s^{-1})
$H\delta_{System}$	1.5	10.6	4273.8	12397	...
$H\gamma_{System}$	1.3	10.7	4521.5	12380	...
He I $\lambda5876_{System}$	0.01	1.2	6120.4	12426	...
He I $\lambda3889_{BAL1}$	8.0	13.2	3991.1	7781	−4619
Ca II K_{BAL1}	8.0	11.1	4037.7	7810	−4590
Ca II H_{BAL1}	5.9	10.9	4071.5	7780	−4620
Na I $D_{BAL1\ Nucleus}$	21.0	20.0	6047.5	7780	−4620
Na I $D_{BAL1(2-5''W)}$	7.3	23.0	6048.5	7840	−4560
Na I $D_{BAL1(2-5''E)}$	7.5	22.0	(6058.3)	...	...
He I $\lambda3889_{BAL2}$	1.8	9.1	3968.5	6130	−6270
Na I $D_{BAL2\ Nucleus}$	1.5	11.8	6015.8	6190	−6210
He I $\lambda3889_{BAL3}$	0.4	5.8	3948.0	4490	−7910
Na I $D_{BAL3\ Nucleus}$	1.1	10.1	5981.5	4460	−7940

[a] Velocities have been obtained using the expression $1 + z = ([c + V]/[c - V])^{0.5}$.
[b] That is, $V_{System} = 12400$ km s^{-1} ($cz = 12{,}670$ km s^{-1}).

§ 3.1), we detected a blue component in the [O II] λ3727; moreover, possibly Hα and [N II] also show a similar/weak blue component (see Table 3 and Fig. 4).

The velocity of each line component, in terms of its absolute velocity and relative to the system velocity, is shown in Table 3 (for the nucleus and the circumnuclear "region I"). While the main component (2) has a velocity consistent with the system velocity, the blue component (1) has a blueshift of about 1000 km s^{-1}. Velocity differences like these (~1000 km s^{-1}) are also found in the double-peak profiles of the emission lines occurring in high and ultraluminous IR galaxies (Heckman et al. 1990; Colina et al. 1991). The interpretation of the line splitting in terms of a biconical flow generated in a large process of star formation ("superwinds") will be discussed in § 4.3.

In "region I" we also found what could be the evidence of a direct relation between a starburst and a BAL system. On the blue side of the blend of Hα and [N II], a secondary peak of these emission lines (system E0) at $V_{E0} = 7941 \pm 80$ km s^{-1} is found (see Table 3 and Figs. 4*a* and 4*b*). This velocity is close to the velocity of the strongest absorption line system BAL1! ($V_{BAL1} = 7787 \pm 110$ km s^{-1} for the nuclear region; see Table 2). The system BAL1 was found in "region I" at a velocity $V_{NaID} = 7840 \pm 120$ km s^{-1} (see Fig. 4*a*). It is important to note that these two features (E0 and BAL1) are more clear and stronger in the subregion between 3″ and 6″ W, far from the contamination of the seeing nuclear disk, and where the broad Hα nuclear component is clearly absent. Moreover, in this region, HK87 also show—in their Figure 8—the system E0 (at low signal-to-noise ratio [S/N]) labeled as a "blue excess in Hα;" and they suggested that this blue excess is evidence for gas outflow. Consequently, we found a new emission line system (E0) with a velocity similar to that of BAL1!

TABLE 3

VELOCITY OF THE EMISSION-LINE COMPONENTS

Line	λ_{obs} (Å)	V (km s^{-1})	$V - V_{System}$ (km s^{-1})
Nucleus (< 1″):			
[O III] $\lambda3727_{[1]}$	3870.0	11262	−1138
[O III] $\lambda3727_{[2]}$	3883.5	12298	−0102
2″–5″ W:			
$H\alpha_{[0]}$	6740.0	7985	−4415
[N II] $\lambda6583_{[0]}$	6759.1	7897	−4503
[O III] $\lambda3727_{[1]}$	3871.0	11320	−1080
$H\alpha_{[1]}$	6814.0	11262	−1138
[N II] $\lambda6583_{[1]}$	(6840.0)	(11435)	...
[O III] $\lambda3727_{[2]}$	3884.0	12327	−0073
$H\alpha_{[2]}$	6835.7	12212	−0188
[N II] $\lambda6583_{[2]}$	6860.0	12327	−0073
[S II] $\lambda6717_{[2]}$	6997.7	12298	−0102
[S II] $\lambda6731_{[2]}$	7012.0	12270	−0130

We found similar properties (e.g., extended BAL1 and E0 systems; see Table 2) on the other side of the nucleus (~2″–5″, in the E direction), though these features are less clear than on the west side. In agreement with HK87, which found that the "*blue excess in* Hα" is present at several positions, for $r < 4''$. They also report that this blue feature only shows a strong extension (more than 5″) to the west.

Finally, in the outer regions (7″–12″), our spectra clearly show a composite nature for the stellar population, mainly: 1) regions with the characteristics of an enhanced population of young stars, with blue continuum excess and nebular emission lines; and 2) regions dominated by old stellar population, with red continuum and absorption lines typical of old stars. These results are in agreement with previous studies of the stellar population in the host galaxy of Mrk 231 (HK87; HN87), in the sense that the *recent* star-formation process has been *very extensive* in this system.

4. DISCUSSION

4.1. *Markarian 231 as a Buried QSO*

There is clear evidence supporting the presence of a non-thermal AGN-type nucleus in Mrk 231. Preuss & Fosbury (1983) detected a very compact (≤1 pc) radio source in the nuclear region of Mrk 231. Also, radio observations by Neff & Ulvestad (1988) show that a variable compact radio source (with an upper limit to the size of ~30 pc), emits almost 50% of the total radio flux measured from the circumnuclear region (size ~2 kpc).

However, if Mrk 231 harbors a "standard" QSO-type nucleus, this has to be obscured very efficiently and/or has to have an atypical spectral energy distribution. Mrk 231 is an X-ray quiet object, with $L_{X[0.5-4.5\,keV]} < 1.44 \times 10^{42}$ ergs s^{-1}

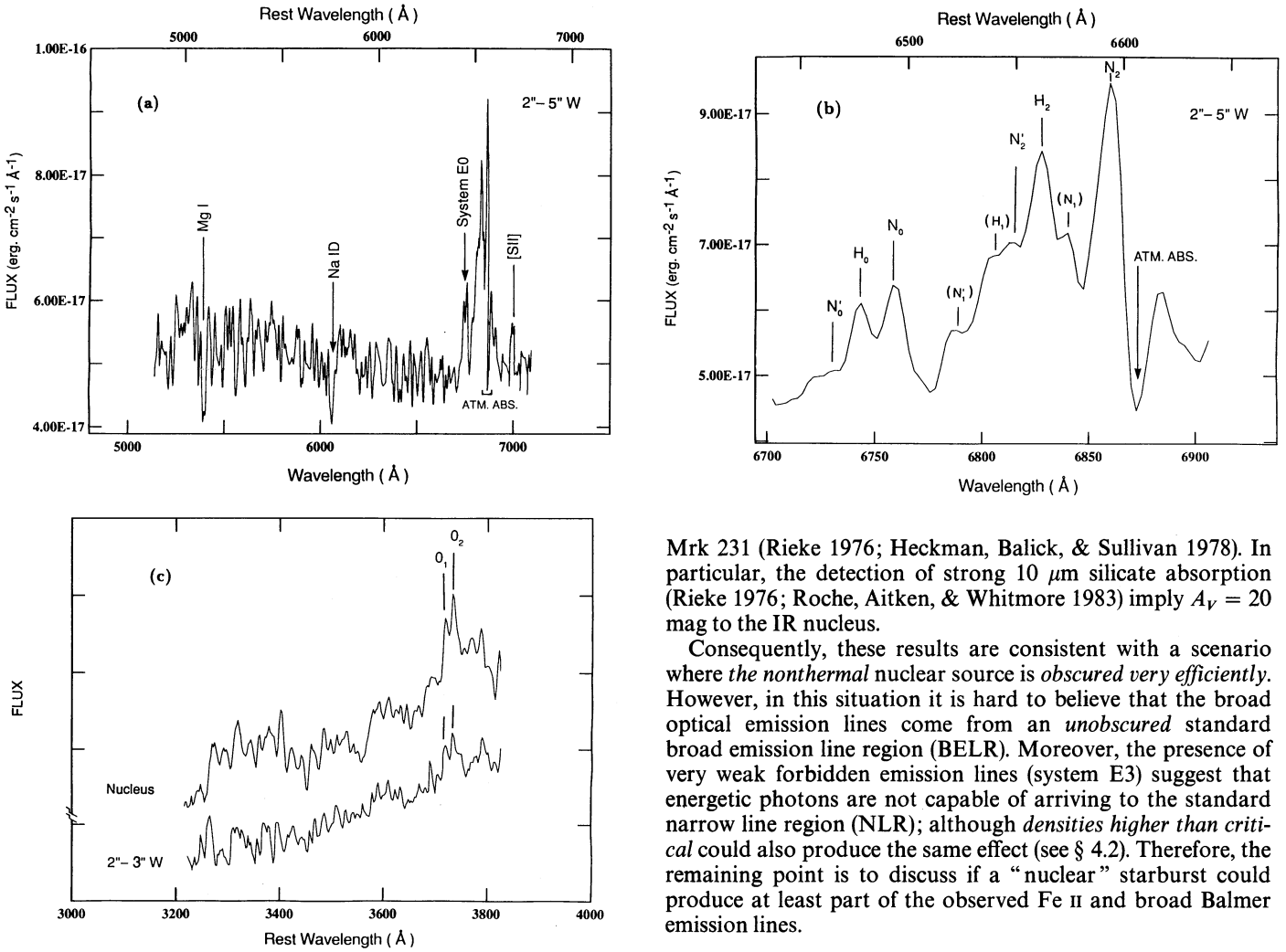

FIG. 4.—Circumnuclear optical spectrum of Mrk 231. (*a*) Hα and [N II] emission line blend (at 2″–5″ W); we also show a second blend of these lines and the absorption lines (see the text). (*b*) Same as (*a*), but with different scale showing in detail the Hα and [N II] blends. (*c*) Double peak [O II] λ3727 emission line.

(Eales & Arnaud 1988; Boller et al. 1992). Dust and molecular gas obscuration do not seem to explain the lack of X-rays, since the column densities needed are higher than those implied by the standard absorption indicators (Eales & Arnaud 1988). On the other hand, in the UV the *IUE* large aperture spectra (Figs. 5*a* and 5*b*) show at low S/N that: 1) the continuum is very steep ($\propto \nu^{-2}$), 2) there is no evidence for the 2200 Å dust extinction feature, and 3) the emission spectrum consists mainly of a narrow and weak Lyα line. These characteristics are typical of starburst galaxies (Kinney et al. 1993). Therefore, it is reasonable to assume that the *IUE* spectrum is associated with the UV flux generated in the nuclear and circumnuclear star forming regions. Moreover, Thompson et al. (1980), BEA77, and Kodaira, Iye, & Nishimura (1979) concluded—from different type of studies—that the "optical" continuum in Mrk 231 is due to *hot young stars* (while the nonthermal nuclear source is obscured by dust).

Furthermore, the IR and radio emission also provide direct evidence for obscuring dust and gas toward the very nucleus of Mrk 231 (Rieke 1976; Heckman, Balick, & Sullivan 1978). In particular, the detection of strong 10 μm silicate absorption (Rieke 1976; Roche, Aitken, & Whitmore 1983) imply $A_V = 20$ mag to the IR nucleus.

Consequently, these results are consistent with a scenario where *the nonthermal* nuclear source is *obscured very efficiently*. However, in this situation it is hard to believe that the broad optical emission lines come from an *unobscured* standard broad emission line region (BELR). Moreover, the presence of very weak forbidden emission lines (system E3) suggest that energetic photons are not capable of arriving to the standard narrow line region (NLR); although *densities higher than critical* could also produce the same effect (see § 4.2). Therefore, the remaining point is to discuss if a "nuclear" starburst could produce at least part of the observed Fe II and broad Balmer emission lines.

4.2. *Markarian 231 as an Extremely Strong* Fe II *Emitter*

The "Fe II problem" of the standard BELR photoionization models is well known. These models do not explain Fe II_{TOT}/Hβ larger than 6, while the observed average is of the order of 10 (see Joly 1991). In extreme cases like Mrk 231, where a Fe II_{OPT}/Hβ ratio of about 8 is measured, the situation is even worse. Detailed photoionization models (Wills, Netzer, & Wills 1985) used to fit the Mrk 231 Fe II flux (Fig. 6) show a clear discrepancy. In Figure 6 we show a fit of one of these models, convolved for a value of FWHM 4800 km s^{-1} (a mean value, between the observed FWHM of Hβ and Hα). One could try to improve this fit by increasing the FWHM of the Fe II emission. However, in this case, the emission of Hβ disappears, while at the same time Hα remains at a very high flux level (and FWHM). This presents a clear example of the problems confronted by the "*pure*" BELR photoionization models when trying to explain the extreme Fe II and the H I Balmer emission.

A *complementary or alternative* point of view is to consider homogeneous clouds in collisional equilibrium at the mid-/low-temperature range (6000–8000 K) and at high densities (10^{12} cm^{-3}). In a warm, high-density gas one expects a high ratio of Fe II_{OPT}/Hβ as a consequence of the differences in the excitation potential among the hydrogen and iron atoms.

Also, according to detailed ionization models (Thompson

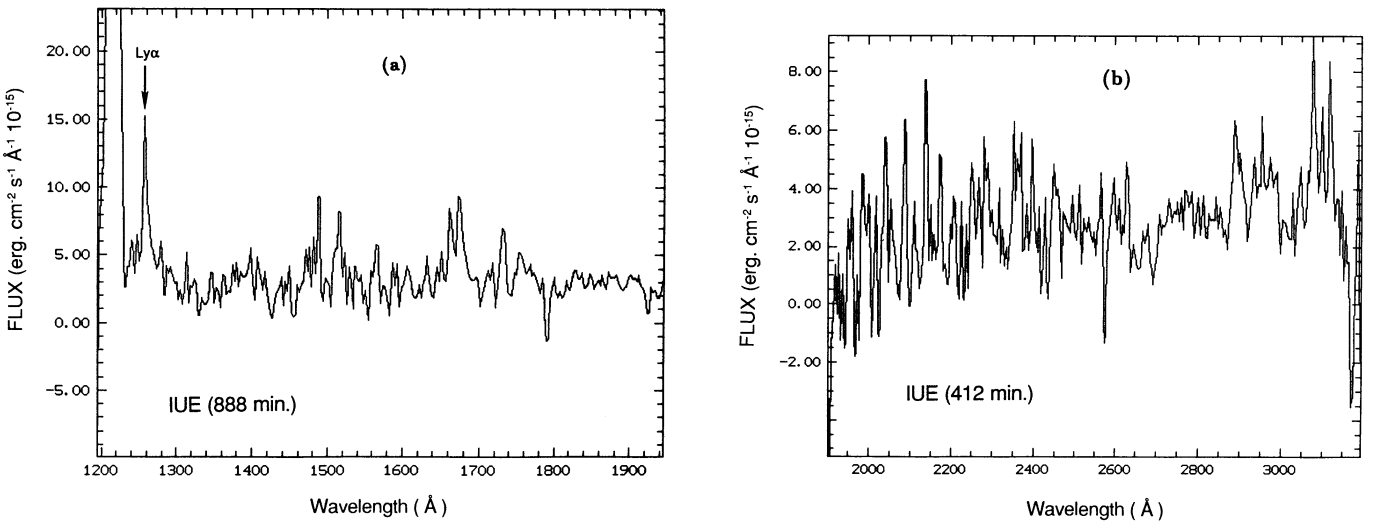

FIG. 5.—UV *IUE* spectrum of Mrk 231. (*a*) *IUE*-SWP spectrum (region λλ1200–2000 Å). (*b*) *IUE*-LWR spectrum (region λλ1900–3200 Å).

1991) the presence of Na I D in emission with an observed intensity of greater than 0.01 that of the Hα emission line (as we obtained for Mrk 231; see Table 1) can only be reproduced if high-density clouds ($N_e = 10^{11}$ cm^{-3}) and column densities $N_H \geq 10^{21}$ cm^{-2} are considered. The need for a high-density medium in Mrk 231 is also in agreement with the observations of an anomalously large Paα/Paβ ratio reported by Cutri et al. (1984). They suggest that the electron density ($N_e \geq 10^{10}$ cm^{-3}) in the BELRs of Mrk 231 is much higher than that typically quoted for standard BELRs in active galaxies.

Starbursts where the *outer shell of the supernovae* (*SN*) *remnants* (SNR) are the *low-ionization* (LIL) *part of the* "*BELR*," have physical conditions (i.e., mid-/low-temperature and high-density; Terlevich et al. 1992) very similar to those needed to reproduce the Na I D intensity, and the increase of the Fe II multiplets with respect to the Balmer lines.

Starburst models predict, in the last stage, a phase dominated by SNs of Type II (8 to 60 Myr, from the initial starburst) where the BELR is fully developed (Terlevich 1992). Furthermore, "strong Fe II emission" from the Type II SNs is expected in this phase. Observations reported by Filippenko (1989) show strong Fe II emission (Fe II [37, 38] λ4570/Hβ ~ 1) for the Type II SN 1987F, supporting the feasibility of this scenario. Moreover, the observations of SN 1987F also show that the peak of the blend "He I λ5876 + Na I λ5892" is consistent with strong Na I λ5892 emission (Filippenko 1989).

In general, this starburst scenario requires ~5–10 SN yr^{-1} (for luminous AGNs; Terlevich et al. 1992), which is a typical value that we expect for the SN event rate in powerful ultraluminous IR galaxies (~3–30 SN yr^{-1}; Heckman et al. 1987; Colina & Pérez-Olea 1992). In particular, for Mrk 231, we can estimate the star-formation rate (SFR) and the rate of SN event ($\nu_{[SNE]}$) using the observed infrared luminosities (Heckman et al. 1990; Colina et al. 1991). If we assume that the starburst contribute at least 50% of the total IR luminosity (Cutri et al. 1984), we obtain the following ranges for the SFR(L_{IR}) and $\nu_{[SNE]}$:

$$800 \leq \mathrm{SFR}(L_{IR}) \leq 1600\ M_\odot\ \mathrm{yr}^{-1};\quad 3.5 \leq \nu_{[SNE]} \leq 7\ \mathrm{yr}^{-1}\ .$$

It is important to note the agreement between these results (very high SFR and $\nu_{[SNE]}$) and the fact that Mrk 231 is an IR galaxy with one of the highest ratios of the IR luminosity to molecular gas content $L_{IR}/M_{CO}(H_2) = 226$!, where this ratio is commonly accepted as a *signature of global starburst activity* (Scoville & Soifer 1991).

In summary, the starburst scenario at the phase of Type II SNs (Terlevich et al. 1992), provides an *alternative and complementary* explanation for at least part of the extreme Fe II emission measured in Mrk 231.

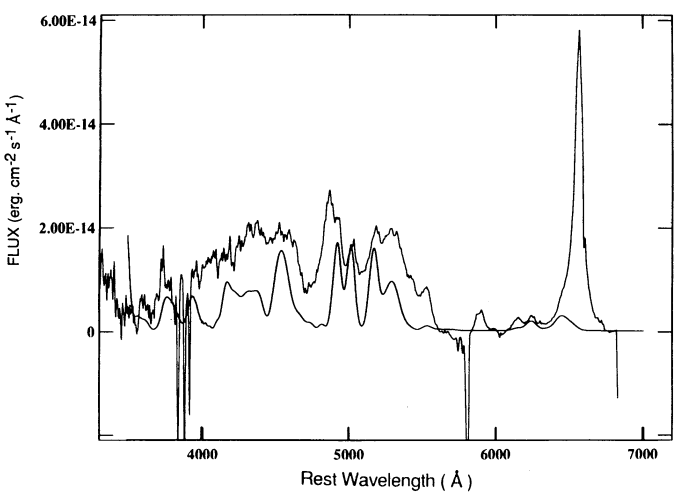

FIG. 6.—Optical nuclear emission spectrum of Mrk 231 superposed with a photoionization model for the Fe II emission (from Wills et al. 1985; see the text).

4.3. *Markarian 231 as a Starburst/Superwind Galaxy*

Further evidence for the existence of an extended nuclear and circumnuclear starburst in Mrk 231 comes from the detection of blue continuum spectra and double peaked emission lines in regions around the nucleus. In particular, for the "region I," we detected blue continuum plus a blue component in the main narrow emission lines (see § 3.2.3). Similar velocity splittings in the [O II] λ3727, and [O III] λ5007 lines have been detected in the "nuclear" region and south of the nucleus, respectively (BEA77; HK87). This line splitting could corre-

spond to two independent kinematical components separated by a projected velocity of about 900–1000 km s^{-1}. Furthermore, this velocity splitting is reminiscent of outflows detected in ultraluminous IR galaxies (Heckman et al. 1990; Colina et al. 1991). On the other hand, the optical continuum in these regions rises towards the blue indicating the possible presence of young hot stars and/or shock mechanism.

Our observations and the previously quoted work clearly show that *outflows*, directly connected with star-forming regions, are common and are located in the nuclear and circumnuclear regions of Mrk 231. Moreover, the conclusion that the IR emission is not dominated by the bright central source (Bregman & Witteborn 1984) also supports the idea of extended starbursts.

On the other hand, the presence of a strong starburst with high SFR and "superwinds" in Mrk 231 is consistent with the "explosive models" that Ostriker & Cowie (1981) proposed to be associated with galaxy formation, where the collective effects of multiple SNs and stellar winds represent efficient conversion of mass into kinetic energy in the ISM ($\sim 10^{58}$ ergs over time scale of 10^7 yr; Colina et al. 1991).

It is important to note that the morphological and kinematic properties of the "structure II" (see § 3.1) are in close agreement with the parameters obtained by Suchkov et al. (1993, private communication) for regions of "shocked *superwind*." In particular, using new hydrodynamic models, they predict interesting structures after 8.3 Myr when the superwind/starburst is in the "blowout" phase: 1) wide *blue arcs* at $r \sim 3$ kpc (as we observed in the "structure II"), which are composed by the outer shocked halo gas, the shocked gas of the galactic disk material, plus the compressed wind material; and 2) narrow "filamentary" structures associated with the flow of material ejected from the starburst and the galactic disk (that arise within the hot bubble). Also, it is interesting to note that at this stage, after 8 Myr, the starburst is probably in the phase of Type II SN (see § 4.2); and SN of Type II are the galactic objects capable to generate the superwind, the superbubble, and the blowout phase (Norman & Ikeuchi 1989).

On the other hand, using the flux of the narrow emission line of Hα measured in the "region I" (see Table 4) we found a lower limit for the number of ionizing photons $N_{ph} \geq 10^{52}$ photons s^{-1}, and this value corresponds to a number of O-type star $N_{O\text{-stars}} \geq 1100$; which is a typical value for star-formation regions (e.g., M82-A, LMC–30 Dor, M101–NGC 5461; see Leitherer 1991). In general, the properties and the extended nature of this area (see § 3.2.3, Adams 1972; HK87; Ulvestad et al. 1981) can be explained mainly by the overlap of extended star-formation areas and associated stellar/SN winds (this suggestion is also supported by the emission-line ratio measured in this region; see below).

TABLE 4

CIRCUMNUCLEAR EMISSION-LINE FLUXES

Lines	F_{obs}[a]	$FWHM_{obs}$ (Å)
2″–5″ W:		
[O I] $\lambda 6300_{[2]}$	0.9	14
$H\alpha_{[0]}$	0.4	12
$H\alpha_{[1]}$	1.4	13
$H\alpha_{[2]}$	4.3	15
[N II] $\lambda 6583_{[0]}$	0.5	12
[S II] $\lambda 6717_{[2]}$	0.8	14
[S II] $\lambda 6731_{[2]}$	0.8	14
$\log([O\ I]\ \lambda 6300/H\alpha)_{[2]}$	−0.68	...
$\log([S\ II]\ \lambda 6724/H\alpha)_{[2]}$	−0.43	...

[a] The fluxes are given in units of 10^{-15} ergs cm^{-2} s^{-1} $Å^{-1}$.

Finally, using the emission-line ratios [O I] λ6300/Hα versus [S II] λ6717 + 6731/Hα for the average extranuclear gas in this "region I" (Table 4), we found that the position of Mrk 231 in this diagram is very close to that obtained by Heckman et al. (1990) for the average of the extranuclear region of IR luminous galaxies with powerful starbursts and superwinds (Arp 220, M82, NGC 6240, and IRAS 00182 − 7112). Consequently, we have shown that both emission-line profiles and emission-line ratios support the *extended starburst/superwind scenario* for Mrk 231.

4.4. *Markarian 231: BAL–Starburst/Superwind Connection*

In "region I" (see §§ 3.1 and 3.2.3) we detect a new emission-line system (E0) (see Fig. 4*a* and Table 3). This system has a blueshifted velocity coincident with that of the strongest broad Na I D absorption line (BAL1). Also, in this region we detected the presence of this BAL1 system. This gives therefore a direct connection between the emission lines and part of the broad absorption line systems. Consequently, it could be the first detection of a direct link between an extended star-formation process and the BAL phenomenon. Furthermore, based on ionization and velocty structure, Rudy, Foltz, & Stocke (1985) concluded that the BAL systems of Mrk 231 must be located more than 150 pc from the continuum source; and if the absorbing gas clouds are located outside the nucleus, then the acceleration mechanism is active over an *immense volume of space*. These properties could be associated with an extensive nuclear/circumnuclear starburst.

On the other hand, a number of theoretical arguments have been given suggesting that "some" QSO/quasar absorption lines could be associated with the material ejected from giant starbursts; i.e., associated to outflow in nuclear/circumnuclear superwinds and in the ejecta of the SNR (see York et al. 1986, 1990; Shapiro & Field 1976; McKee & Ostriker 1977; Bregman 1980; Ikeuchi & Ostriker 1986; Lake 1988; Norman & Ikeuchi 1989; Scoville & Norman 1988; Scoville 1992; Dyson, Perry, & Williams 1992). On the other hand, spectral observations of SN 1987F (Filippenko 1989) show strong blueshift in the Na I D absorption line plus strong blue asymmetry in the Hα emission line.

Consequently, under the extended starburst scenario, a mixture of these outflow mechanisms (i.e., ejecta of SNRs in young star clusters, hot superbubbles, and filamentary superwinds) could explain 1) the kinematical coincidence between the strongest of the three BAL systems and some emission line regions associated with star-forming regions and 2) the possible extended nature of the BAL1 system. However, it is important to note that there are also different classes and combinations of QSO absorptions lines and they may not represent "homogeneous physical processes" (i.e., overlapping outflow from nuclear star-forming regions with galactic ejecta, radio lobes, halos, etc.; see York 1988). Therefore, high spatial resolution observations (in the nuclear and circumnuclear regions of Mrk 231) are needed to study in detail these BAL systems and their relation with the BELR. In particular, it is interesting to note that the proposition that the Fe II emission is originated in the outer shell of the SNR is in good agreement with the conclusion that in some strong Fe II emitters this

emission is *not occulted* by the BALR (see Wampler 1985; Pettini & Boksenberg 1985; Turnshek et al. 1988).

It is important to note that, recently, Boroson & Meyers (1992) found important results in their study of BAL QSOs. They found that the interesting class of "low-ionization" BAL QSO are mainly IR QSOs with unusual properties: strong Fe II/Hβ plus Na I λ5892 emission, weak [O III] λ5007 emission, blue asymmetry in the Hα emission, and they are all radio-quiet objects (Mrk 231 is also included in this group). These results can be explained in the framework of the starburst scenario that we discussed for Mrk 231. In particular, the weak emission in [O III] λ5007, the strong Fe II/Hβ plus Na I λ5892 emission, could be a consequence of high densities in the outer shell of the SNR (see § 4.2); and the blue asymmetry in Hα could be the result of the emission associated with the starburst/BAL system. Also, these objects could be considered IR active galaxies at different stages of the starburst phase and/or merger process. In this scenario, interacting ultraluminous IR galaxies that have reached the phase of fusion of their nuclei (and/or the formation of a supermassive black hole) become a QSO or even a radio galaxy (Barnes & Hernquist 1991; Kormendy & Sanders 1992), probably at the end phase of a strong starburst.

Finally, it is important to note (in relation to the merger scenario for Mrk 231; see § 3.1) that some of the nuclear properties (e.g., $M_K = -24.7$ and extreme red color $[V - K] \sim 4$) show a remarkable agreement with the typical values observed in *giant elliptical* galaxies (see Cutri et al. 1984). Moreover, the mean brightness profile of Mrk 231 shows the typical $r^{1/4}$ profile (HK87). Consequently, different properties of Mrk 231 are in good agreement with the characteristics of a merger remnant showing elliptical-like features. Furthermore, this merger process is probably the main triggering mechanism that can explain the origin of the high concentration of molecular gas observed in the nuclear/circumnuclear regions of Mrk 231 (SEA87) and also the origin of the extended starburst plus the obscured nonthermal nuclear source (Sanders et al. 1988a; Barnes & Hernquist 1991).

5. SUMMARY AND CONCLUSIONS

We have studied the nuclear and circumnuclear region of Mrk 231, which is the nearest object of the important group of ultraluminous IR galaxies with extreme Fe II emission and broad absorption lines. The main results can be summarized as follows.

1. The characteristics of the UV and optical spectrum, strong Fe II optical emission, broad Balmer and Na I lines, weak high-excitation lines, double-peaked optical emission lines, steep UV spectrum, and weak Lyα line are associated "mainly" to nuclear and circumnuclear starbursts.

2. In the star-forming circumnuclear region "region I" (located at $\sim 2''$–$5''$ west of the nucleus) we detected a new emission line system (E0) with a velocity ($V_{E0} = 7941 \pm 80$ km s^{-1}) similar to the nuclear system BAL1 ($V_{BAL1} \sim 7800$ km s^{-1}), the strongest of the three absorption line systems. Also, in this "region I" we detected the probable presence of this BAL1 system ($V_{NaID} = 7840 \pm 120$ km s^{-1}). This therefore gives a direct kinematical connection between the emission-line regions and part of the broad absorption-line systems. Consequently, it shows a direct link between the star-formation process and the BAL phenomenon.

These results are consistent with a scenario where this ultraluminous IR galaxy has a composite nature in the nuclear region, as the result of an advanced merger process, and where the starburst (with superwind/superbubble and Type II SN) is the *dominant* source of nuclear/circumnuclear energy and the nonthermal AGN remains strongly obscured.

In conclusion, we interpret the *extreme properties* of Mrk 231, i.e., 1) extreme IR emission associated with a powerful starburst with superwind/SN plus a strongly obscured nonthermal AGN, 2) advanced merger morphology showing elliptical-like features, and 3) strong Fe II emission plus BAL systems, as the "*probable*" *characteristics or signature of a young IR QSO.*

It is a pleasure to thank D. M., Pedro Rodriguez, Anatoly Suchkov, Roberto Terlevich, and Zlatan Tsvetanov for many stimulating discussions. We would like to express our gratitude to the staff members and observing assistants of La Palma and KPNO Observatories, especially Richard Green, for carrying out some of the observations reported in this paper. We wish to thank the referee for valuable critical comments. S. L. was supported in part by an AURA/STScI grant and from Conicet (Argentina).

REFERENCES

Adams, T. F. 1972, ApJ, 176, L1
Adams, T. F., & Weedman, D. W. 1972, ApJ, 173, L19
Arakelian, M. A., Dibai, E., Esipov, V., & Markarian, B. 1971, Astrofizika, 7, 177
Armus, L., Heckman, T. M., & Miley, G. 1989, ApJ, 347, 727
———. 1990, ApJ, 364, 471
Baan, W. A. 1985, Nature, 315, 26
Barnes, J. E., & Hernquist, L. 1991, ApJ, 370, L65
———. 1992, Nature, 360, 715
Bevington, P. 1969, Data Reduction and Error Analysis for the Physical Sciences (New York: McGraw-Hill)
Boksenberg, A., Carswell, R., Allen, D., Fosbury, R., Penston, M., & Sargent, W. 1977, MNRAS, 178, 451 (BEA77)
Boller, Th., et al. 1992, A&A, 261, 57
Boroson, T., & Meyers, K. 1992, ApJ, 397, 442
Boroson, T., Meyers, K., Morris, S., & Persson, S. E. 1991, ApJ, 370, L19
Bregman, J. N. 1980, ApJ, 236, 577
Bregman, J., & Witteborn, K. 1984, ApJ, 281, L17
Colina, L., Lípari, S., & Macchetto, F. 1991, ApJ, 379, 113
Colina, L., & Perez-Olea, D. 1992, MNRAS, 259, 709
Cutri, R. M., Rieke, G. H., & Lebofsky, M. J. 1984, ApJ, 287, 566
Djorgovski, S., & Weir, N. 1990, ApJ, 351, 343
Dyson, J. E., Perry, J., & Williams, R. 1992, in Testing the AGN Paradigm, ed. S. Holts, S. Neff, & M. Urry (New York: AIP), 548
Eales, S. A., & Arnaud, K. A. 1988, ApJ, 324, 193
Filippenko, A. 1989, AJ, 97, 726
Hamilton, D., & Keel, W. 1987, ApJ, 321, 211 (HK87)
Heckman, T. M. 1990, in IAU Colloq. 124: Paired and Interacting Galaxies, ed. J. W. Suletic, W. C. Keel, & C. M. Telesco (NASA CP 3098), 359
———. 1991, in Massive Stars in Starbursts, ed. C. Leitherer, N. R. Walborn, T. M. Heckman, & C. A. Norman (Cambridge: Cambridge Univ. Press), 289
———. 1992, in Testing the AGN Paradigm, ed. S. Holts, S. Neff, & M. Urry (New York: AIP), 595
Heckman, T. M., Armus, L., & Miley, G. 1987, AJ, 93, 276
———. 1990, ApJS, 74, 833
Heckman, T. M., Balick, B., & Sullivan, W., III 1978, ApJ, 224, 475
Hutchings, J. B., & Neff, S. G. 1987, AJ, 92, 14 (HN87)
———. 1988, AJ, 96, 1575
———. 1991, AJ, 101, 434
Ikeuchi, S., & Ostriker, J. P. 1986, ApJ, 301, 522
Joly, M. 1991, A&A, 242, 49
Kinney, A., Bohlin, R., Calzetti, D., Panagia, N., & Wyse, R. 1993, ApJS, 86, 5
Kodaira, K., Iye, M., & Nishimura, S. 1979, PASJ, 31, 451
Kormendy, J., & Sanders, D. 1992, ApJ, 390, L53
Lake, G. 1988, ApJ, 327, 99
Leech, K., et al. 1989, MNRAS, 240, 349
Leitherer, C. 1991, in Massive Stars in Starbursts, ed. C. Leitherer et al. (Cambridge: Cambridge Univ. Press), 1

Lípari, S., Bonatto, Ch., & Pastoriza, M. 1991a, MNRAS, 253, 19
Lípari, S., Macchetto, F., & Golombek, D. 1991b, ApJ, 366, L65
Lípari, S., Terlevich, R., & Macchetto, F. 1993a, ApJ, 406, 451
Lípari, S., Tsvetanov, Z., & Macchetto, F. 1993b, ApJ, 405, 186
McKee, C. F., & Ostriker, J. P. 1977, ApJ, 218, 148
Melnick, J., & Mirabel, F. 1990, A&A, 231, L19
Nandy, K., Morgan, D., Willis, D., Wilson, R., & Gondhalekar, P. 1981, MNRAS, 196, 955
Neff, S. G., & Ulvestad, J. S. 1988, AJ, 96, 841
Norman, C., & Ikeuchi, S. 1989, ApJ, 345, 372
Ostriker, J. P., & Cowie, L. L. 1981, ApJ, 243, L127
Pettini, M., & Boksenberg, A. 1985, ApJ, 294, L73
Preuss, E., & Fosbury, R. A. 1983, MNRAS, 204, 783
Rieke, G. H. 1976, ApJ, 210, L16
———. 1992, in Connections between Active Galactic Nuclei and Starburst Galaxies, ed. A. Filippenko (Provo: Brigham Young Univ.), 61
Rieke, G. H., Lebofsky, M., Thompson, R., Low, F., & Tokunaga, A. 1980, ApJ, 238, 24
Rieke, G. H., & Low, F. J. 1972, ApJ, 176, L95
———. 1975, ApJ, 200, L67
Rieke, G. H., et al. 1985, ApJ, 290, 116
Roche, P., Aitken, D., & Withmore, B. 1983, MNRAS, 205, 21P
Rowan-Robinson, M., et al. 1991, Nature, 351, 719
Rudy, R., Foltz, C., & Stocke, J. 1985, ApJ, 288, 531
Sanders, D. B. 1992, in Connections between Active Galactic Nuclei and Starburst Galaxies, ed. A. Filippenko (Provo: Brigham Young Univ.), 303
Sanders, D. B., Soifer, B. T., Elias, J. H., Madore, B. F., Matthews, K., Neugebauer, G., & Scoville, N. Z. 1988a, ApJ, 325, 74
Sanders, D. B., Soifer, B. T., Elias, J. H., Neugebauer, G., & Matthews, K. 1988b, ApJ, 328, L35
Sanders, D. B., Young, J. S., Scoville, N. Z., Soifer, B. T., & Danielson, G. E. 1987, ApJ, 312, L5 (SEA87)
Scoville, N. 1992, in Connections between Active Galactic Nuclei and Starburst Galaxies, ed. A. Filippenko (Provo: Brigham Young Univ.), 159
Scoville, N., & Norman, C. 1988, ApJ, 332, 163
Scoville, N., & Soifer, B. T. 1991, in Massive Stars in Starbursts, ed. C. Leitherer, N. R. Walborn, T. M. Heckman, & C. A. Norman (Cambridge: Cambridge Univ. Press), 233
Shapiro, P. R., & Field, G. B. 1976, ApJ, 205, 762
Soifer, B. T., Sanders, D., Madore, B. F., Neugebauer, G., Danielson, G. E., Elias, J. H., Lonsdale, C. J., & Rice, W. L. 1987, ApJ, 320, 238
Soifer, B. T., Sanders, D., Madore, B. F., Neugebauer, G., Danielson, G. E., Lonsdale, C. J., Madore, B. F., & Persson, S. E. 1986, ApJ, 303, L41
Terlevich, R. 1992, in Connections between Active Galactic Nuclei and Starburst Galaxies, ed. A. Filippenko (Provo: Brigham Young Univ.), 133
Terlevich, R., Tenorio-Tagle, G., Franco, J., & Melnick, J. 1992, MNRAS, 255, 713
Thompson, I., Landstreet, J., Stockman, H., Angel, J., & Beaver, E. 1980, MNRAS, 192, 53
Thompson, K. L. 1991, ApJ, 374, 496
Turnshek, D., Foltz, C., Grillmair, C., & Weyman, R. 1988, ApJ, 325, 651
Ulvestad, J. S., Wilson, A., & Sramek, R. A. 1981, ApJ, 247, 419
Wampler, E. J. 1985, ApJ, 296, 416
Wills, B., Netzer, H., & Wills, D. 1985, ApJ, 288, 94
York, D. G. 1988, in QSO Absorption Lines, ed. C. Blades, D. Turnshek, & C. Norman (Cambridge: Cambridge Univ. Press), 227
York, D. G., et al. 1990, ApJ, 351, 412
York, D. G., Dopita, M., Green, R., & Bechtold, J. 1986, ApJ, 311, 610